

# Absence of Diffusion in an Interacting System of Spinless Fermions on a One-dimensional disordered lattice

Yevgeny Bar Lev,<sup>1</sup> Guy Cohen,<sup>1,2</sup> and David R. Reichman<sup>1</sup>

<sup>1</sup>*Department of Chemistry, Columbia University, New York, New York 10027, USA\**

<sup>2</sup>*Department of Physics, Columbia University, New York, New York 10027, USA*

We study the infinite temperature dynamics of a prototypical one-dimensional system expected to exhibit many-body localization. Using numerically exact methods, we establish the dynamical phase diagram of this system based on the statistics of its eigenvalues and its dynamical behavior. We show that the nonergodic phase is reentrant as a function of the interaction strength, illustrating that localization can be reinforced by sufficiently strong interactions even at infinite temperature. Surprisingly, within the accessible time range, the ergodic phase shows subdiffusive behavior, suggesting that the diffusion coefficient vanishes throughout much of the phase diagram in the thermodynamic limit. Our findings strongly suggest that Wigner–Dyson statistics of eigenvalue spacings may appear in a class of ergodic but subdiffusive systems.

The interplay between particle interactions and disorder may lead to complex emergent phenomena, especially in one-dimensional systems where the influence of both effects is maximized. Non-interacting particles in a one-dimensional disordered system exhibit Anderson localization [1] which results in insulating, nonergodic behavior. Coupling the localized system to phonons will restore ergodicity and transport with a peculiar dependence on the temperature, a phenomenon known as variable-range hopping [2]. In the absence of phonons or coupling to any other degrees of freedom it was generally believed that the inter-particle interactions conspire to induce transport and restore ergodicity [3], although the opposite was also suggested in a later study [4]. Nevertheless, using self-consistent perturbation theory in the interaction term, it has recently been suggested that the localized phase survives finite interactions [5, 6]. Moreover, *the many-body* spectrum is predicted to have a mobility edge separating the localized and metallic states, similar to the one-particle mobility edge in three-dimensional systems [7]. For lattice models where the energy density is bounded, it has been proposed that a range of parameters might exist for which *all* the many-body eigenstates are localized, such that the many-body localization (MBL) transition persists at infinite temperatures [8]. This argument has recently been made more precise [9, 10]. The existence of a nonergodic phase for strong disorder and weak interactions has been rigorously proven for zero particle density [11] and for an infinite chain of spins [12]. However, currently there are no rigorous results for the ergodic phase or the MBL transition itself. Although realizing a truly isolated physical system is impossible, recent experiments in cold atom systems come very close to this idealized limit [13–15].

The MBL transition is a dynamical transition between a nonergodic and an ergodic phase, and it has no manifestation in static thermodynamic quantities. Its unconventional nature has attracted many researchers. In particular, the dynamical features of the transition which

have been studied are the dc conductivity [16–18] and dynamical correlations in the  $t \rightarrow \infty$  limit [19]. In all of these studies exact diagonalization (ED) has been used, effectively restricting the accessible system sizes to about 16 sites. This fact poses serious limitations on the interpretation of the results. In particular, the evaluation of the dc conductivity depends on a careful extrapolation to the thermodynamic limit [20], while for systems of finite length  $L$ , dynamics in the  $t \rightarrow \infty$  limit are dominated by finite size effects and may have little in common with the behavior of  $L \rightarrow \infty$  system. Another measure which has been used to study the MBL transition is the distribution of spacings of the many-body eigenvalues. At the transition the distribution is expected to cross over from a Poisson to a Wigner–Dyson distribution [8, 19]. For one-particle systems, it has been conjectured in Ref. [21] that quantum systems with fully chaotic classical analogs will exhibit a Wigner–Dyson distribution of eigenvalue spacing. It was later shown that the Wigner–Dyson distribution of *many-body* eigenvalue spacing is generic and connected to *quantum* non-integrability [22, 23]. Nevertheless, the connection between non-integrability and transport properties is not rigorously understood. For clean, translationally invariant systems, non-integrability generally results in the disappearance of ballistic transport [24–26], however for disordered *many-body* systems its implications have not been fully explored. A number of numerically exact studies have examined the dynamics directly. It has been shown that time-dependent density matrix renormalization group (tDMRG) becomes efficient for highly localized systems [27]. For weak interactions a logarithmic growth of entanglement entropy as a function of time has been observed [27, 28] and later explained [29–31]. Entanglement entropy is however a non-local quantity with no direct relation to the measurable dynamical properties of the system. Two of the authors in a previous work directly observed nonergodicity by studying the relaxation of the on-site particle density, in a study limited to weak interactions [9]. In

a very recent study quantum revivals of the local density were used to differentiate between the Anderson and MBL localized phases [32].

In this letter we explore the dynamical phase diagram of a system of interacting spinless fermions in a one-dimensional disordered lattice via the examination of the spectral properties and the transport of correlations in the system. The Hamiltonian we consider is given by

$$H = -t \sum_i \left( \hat{c}_i^\dagger \hat{c}_{i+1} + \hat{c}_{i+1}^\dagger \hat{c}_i \right) \quad (1)$$

$$+ V \sum_i \left( \hat{n}_i - \frac{1}{2} \right) \left( \hat{n}_{i+1} - \frac{1}{2} \right) + \sum_i h_i \left( \hat{n}_i - \frac{1}{2} \right),$$

where  $t$  (which we set to one) is the hopping matrix element,  $V$  is the interaction strength and  $h_i$  are random on-site fields independently distributed on the interval  $h_i \in [-W, W]$ . Note that by using the Jordan–Wigner transformation, this model can be exactly mapped onto the XXZ model. Extending the model (1) to a non-integrable (zero field) version (e.g. the model used in Ref. [8]) produces only *quantitative* and not qualitative changes to our conclusions. We therefore focus on (1). For lattice models with a finite number of states per site, the energy density is bounded, which renders the infinite temperatures limit meaningful. To simplify the discussion we follow Ref. [8] and consider only the infinite temperature limit throughout this Letter.

To establish the full dynamical phase diagram using eigenvalue statistics we repeat the analysis of Ref. [8] for a large set of parameters ( $1 \leq W \leq 7$  and  $0.5 \leq V \leq 10$ , a total of 120 points). For this purpose we obtain the eigenvalues of the Hamiltonian (1) for system sizes  $L = 10, 12$  and  $14$  and calculate the metric  $r_n = \min(\delta_n, \delta_{n-1}) / \max(\delta_n, \delta_{n-1})$ , where  $\delta_n \equiv E_n - E_{n+1}$  is the difference between adjacent eigenvalues. This metric is then averaged over all states and disorder realizations (100 realizations were sampled) and is used to differentiate between Wigner–Dyson ( $r = 0.529$ ) and Poisson statistics ( $r = 0.386$ ) of the eigenvalue spacing [8]. It is assumed that the metric  $r(W, V)$  flows to the Wigner–Dyson value in the thermodynamic limit for the ergodic parts of the phase diagram, and similarly to the Poisson value for nonergodic regions. The phase boundary will therefore correspond to points which are “stationary” under scaling of system size. Note that the phase boundaries have to be taken with care; due to the severe limitation on the available system sizes we cannot perform a reliable extrapolation of this procedure to the thermodynamic limit.

In Fig. 1, the resulting phase diagram is presented. A surprising feature of the diagram is the re-entrant behavior of the nonergodic glassy phase. This feature was overlooked in previous studies, which examined only one constant interaction cut through the diagram [8, 19] or

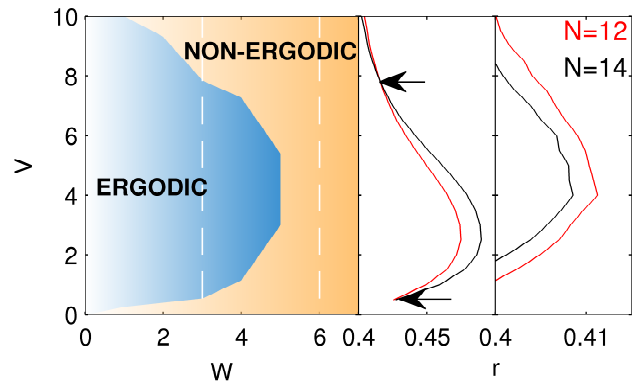


Figure 1: (Color online) Dynamical phase diagram at infinite temperature, as obtained from the spectral fluctuations of the studied model. The dashed white lines correspond to cuts through the phase diagram presented on the right panel. The right panel demonstrates the determination of the phase diagram based on spectral fluctuation analysis of two system sizes,  $N = 12$  and  $N = 14$ . The phase boundary is determined from the crossing of the red (grey) and black lines, as designated by the arrows. The faded region on the left indicates a region of substantial finite size effects.

for weak interactions [32]. It should be noted that in Ref. [33], a suggestion that reentrance may occur in MBL systems was put forward. The re-entrant behavior suggests that sufficiently strong interactions can enhance rather than destroy localization, a phenomena somewhat reminiscent of the Mott transition occurring at low temperatures. Note that while the *clean* system is *insulating* at zero temperature for  $V/t > 2$  [34], it exhibits *diffusive* transport at infinite temperature [35–38]. Therefore, it is the disorder which facilitates localization.

As discussed above, Wigner–Dyson statistics of the level spacing suggest that the system is non-integrable, but for a disordered interacting system there are no established implications for the dynamics. Therefore, it is interesting to examine the dynamics directly across the entire phase diagram. For this purpose, we have used a combination of ED and tDMRG techniques to evaluate the density-density correlation function at infinite temperature,

$$C_{ij}(t) = \frac{1}{Z} \text{Tr} \delta \hat{n}_i(t) \delta \hat{n}_j(0), \quad (2)$$

where  $\delta \hat{n}_i \equiv \hat{n}_i - 1/2$  and  $Z$  is the dimension of the Hilbert space. To eliminate boundary effects it would be preferable to excite the system in the middle of the chain. However, to make the best use ED, which is limited to small system sizes, we instead use open boundary conditions and excite the system at one boundary. This allows for the study of transport over the entire system length, effectively increasing the accessible times. In particular, when the excitation has traveled sufficiently far from the boundary, it is expected that the dynamical charac-

teristics will approach those of the bulk and the initial position of the excitation will be irrelevant. We have confirmed this by exciting the system from its center (data not shown). To quantify the transport of correlations we define

$$\sigma^2(t) = \sum_{n=0}^{L-1} n^2 (C_{n0}(t) - C_{n0}(0)). \quad (3)$$

This quantity measures the *spreading* of correlations analogously to the mean square displacement of a diffusing particle. A similar quantity based on the one-time density ( $\hat{n}_i(t)$ ) has been studied extensively in clean systems out-of-equilibrium [38, 39]. However, such quantities cannot be directly used in equilibrium where any one-time operator is conserved. We therefore consider the spreading of two-time correlations encoded by (3)[40]. The nature of the transport is assessed by examining the finite time dynamical exponent,

$$\alpha(t) \equiv \frac{d \ln \sigma^2(t)}{d \ln t}, \quad (4)$$

which has values  $\alpha(t \rightarrow \infty) = 2$  for ballistic transport and  $\alpha(t \rightarrow \infty) = 1$  for diffusive transport. For finite systems, asymptotic time dynamics will be determined by finite size effects such as reflections from the boundaries. Since we are only interested in the bulk transport of correlations, we limit the considered times to the time  $t_*$  during which the existence of the boundary opposite to the initial excitation has no effect on  $\sigma$ . Until this horizon time, the dynamics will not depend on the simulated system size, since the infinite temperature initial conditions are identical for all system sizes. To determine  $t_*$  we evaluate the spreading of correlations for different system sizes (here  $L = 10, 12$  and  $14$  unless otherwise stated) for every parameter set of the Hamiltonian.  $t_*$  is then taken to be the longest time up to which  $L = 12$  and  $L = 14$  exhibit the same dynamics within the chosen accuracy.

In Fig. 2 this procedure is exemplified for two parameter sets corresponding to the ergodic and nonergodic phases. The horizon time,  $t_*$ , is naturally much longer for the nonergodic phase. For the chosen parameter sets it varies in the range  $5 < t_* < 100$ . There are two interesting dynamical differences between the ergodic and nonergodic phases: although similar computer time was used in the two cases, it is clear that it is significantly harder to converge the averaging of  $\sigma^2(t)$  in the nonergodic phase, as can be seen by the fluctuations of the  $\sigma^2(t)$  in Fig. 2. Another clear difference is the appearance of oscillations in  $\sigma^2(t)$  inside the nonergodic phase, with a period of about  $T \approx 3$ . This period depends neither on the disorder strength nor the interaction, and is related to oscillations of particles effectively localized to lattice sites.

To extract the dynamical exponent  $\alpha$  (4) we first extract the horizon time  $t_*$  for every data point in the

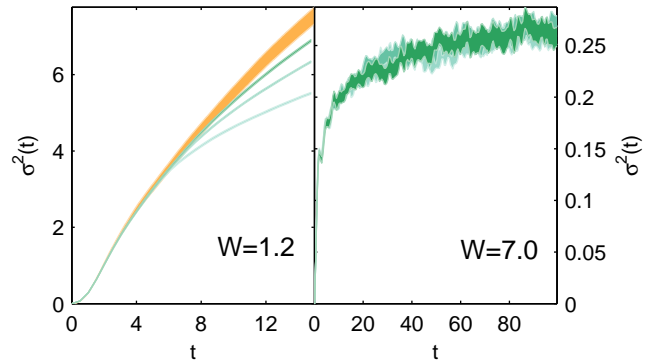


Figure 2: (Color online) Finite size scaling of the dynamical data obtained for various systems sizes at infinite temperature. Darker colors represent larger systems. The left panel shows  $\sigma^2(t)$  as a function of time, for  $V = 2$ , and  $W = 1.2$  and system sizes  $L = 12, 14$  and  $16$  using ED (from bottom) and  $L = 24$  using DMRG (top). The right panel shows  $\sigma^2(t)$  for  $W = 7$  and system sizes  $L = 10, 12$  and  $14$ . Shaded areas designate uncertainty bounds.

phase diagram, and subsequently evaluate the logarithmic derivative of  $\sigma^2(t)$  at  $t_*$  using the procedure illustrated in the left panel of Fig. 3. Repeating the procedure for 24 different parameter points and interpolating gives a rough dynamical “phase diagram” on the right panel of Fig. 3. Phase boundaries cannot be reliably determined by this methodology, since the dynamical exponents obtained are not asymptotic. For the MBL transition scenario advocated in Ref. [6] the ergodic phase is diffusive, which would correspond to an asymptotic dynamical exponent of  $\alpha(t \rightarrow \infty) = 1$  while the nonergodic phase is insulating and should correspond to  $\alpha(t \rightarrow \infty) = 0$ . Surprisingly, the dynamical phase diagram of Fig. 3 has a vanishingly small part with a dynamical exponent close to one. This region corresponds to the weak localization regime, where the *non-interacting* localization length is larger than the size of the simulated system. Interestingly, the contours of equal dynamical exponents retrace the phase diagram of Fig. 1, exhibiting a similar re-entrant behavior. The strong localization seen at Fig. 3 for very weak disorder and strong interaction is an edge effect and is *irrelevant* to the physics of many-body localization. By exciting the system from its center, using tDMRG and system size 32 (for  $W = 4$  and  $V = 10$ , data not shown) we have verified that the re-entrant behavior is *not* influenced by this effect and is a feature that is expected to survive extrapolation to the thermodynamic limit.

In Figs. 2 and 3 we used tDMRG [41–44] to access larger system sizes wherever possible. Surprisingly, for the purposes of this work tDMRG is superior to ED only within a narrow parameter regime characterized by weak disorder [45]. For example, as illustrated in Fig. 3, it

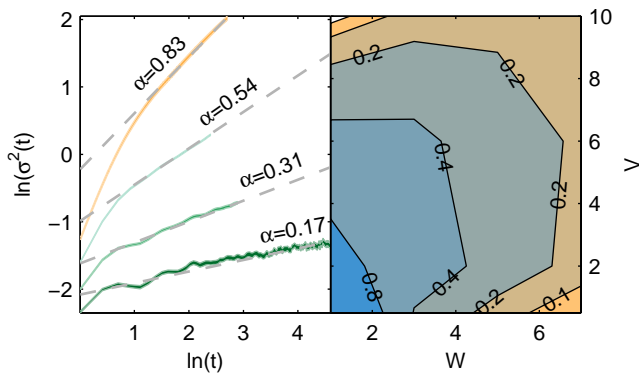


Figure 3: (Color online) Dynamical phase diagram obtained from the dynamical exponents of correlation spreading. The left panel explains the determination of the dynamical exponents from the log-log plot of  $\sigma^2(t)$ . The system sizes which were used  $L = 14$ ,  $V = 2$  and  $W = 3, 5, 7$  (from top to bottom) using ED and  $L = 24$ ,  $V = 2$  and  $W = 1.2$  using tDMRG (top, orange). Shaded areas designate uncertainty bounds. The dynamical exponents are extracted from the slope of the dashed gray lines. The right panel presents the dynamical exponents as a contour plot which interpolates between 24 different parameter points. The text on the contour lines corresponds to the dynamical exponents. Note that due to edge effect discussed in the text the  $W$  axis starts from  $W = 1$  in the right panel.

enables the demonstration of sub-diffusion at very weak disorder,  $W = 1.2$  for which the *non-interacting* localization length is larger than the system sizes accessible to us within ED.

An interesting question which remains is how the *finite time* dynamical exponents  $\alpha(t)$  calculated in this Letter change in the limit of  $t \rightarrow \infty$ . For classical fluids close to the glass transition the typical scenario is slow subdiffusive transport followed by a transition to diffusion; this, however, requires an additional time-scale for which such acceleration of transport (de-caging) occurs [46]. For some parameter choice this time scale can be made arbitrarily small. In our simulations we do not see the appearance of such a time scale even for very weak disorder; throughout the phase diagram  $\alpha(t)$  (averaged over the oscillations) is a decreasing function of time. If this is indeed the case, it implies that transport is subdiffusive throughout the entire phase diagram. Although for small disorder strength the validity time becomes short, making the determination of  $\alpha(t)$  less reliable, the overall tendency of  $\alpha(t)$  to decrease with time throughout the entire phase diagram invites one to *speculate* that the small diffusive region occurring for small disorder and small interaction will vanish in the thermodynamic limit, in the absence of coupling to additional degrees of freedom (such as phonons). We do not have access to the  $t \rightarrow \infty$  limit, but within the attainable timescales we can observe that  $\alpha(t)$  seems to vary contin-

uously across the ergodic–nonergodic transition. Moreover, although fits to logarithmic relaxation appear to be more appropriate in the nonergodic phase, we stress that we cannot clearly distinguish between logarithmic relaxation and weak sub-diffusion (note that logarithmic relaxation still yields  $\alpha(t \rightarrow \infty) = 0$ ) without accessing significantly larger timescales. While we do not show this, logarithmic behavior is consistent with at least some of the data. Both scenarios imply a vanishing diffusion coefficient in the thermodynamic limit.

In summary, we have investigated the dynamical phase diagram of a one-dimensional, spinless fermionic model with short-range interactions and disordered potential. The phase diagram was obtained both by analysis of the distribution of the eigenvalues spacing and the correlations transport in the system. We showed that the nonergodic phase is re-entrant for sufficiently strong interactions which implies that in this part of the phase diagram disorder and interactions reinforce localization. Moreover the phase diagram is predominantly subdiffusive for accessible times. If this behavior persists asymptotically it implies the absence of diffusion in the thermodynamic limit and for any finite disorder strength. Nevertheless, the dynamical phase diagram is composed of an ergodic, but subdiffusive phase and a nonergodic glassy phase. Our findings imply that Wigner–Dyson statistics alone do not rule out subdiffusive behavior. Interestingly, subdiffusive behavior was recently experimentally observed for bosons at low temperatures [47]. It would be of great interest to explore the possibility of the existence of a broad class of quantum non-integrable systems which show subdiffusive behavior.

We would like to thank M. Schiró for many enlightening and helpful discussions. This work used the Extreme Science and Engineering Discovery Environment (XSEDE), which is supported by National Science Foundation Grant No. OCI-1053575. DMRG calculations were performed using the ITensor library, <http://itensor.org>. This work was supported by the Fulbright Foundation and by Grant No. NSF-CHE-1213247.

*Note.* During the review process a number of works supporting the existence of the subdiffusive phase have appeared [48–50]. Also the strongly interacting nonergodic phase predicted in this Letter was observed experimentally [51].

\* Electronic address: yb2296@columbia.edu

- [1] P. W. Anderson, Phys. Rev. **109**, 1492 (1958).
- [2] N. F. Mott, Phil. Mag. **19**, 835 (1969).
- [3] L. Fleishman, D. C. Licciardello, and P. W. Anderson, Phys. Rev. Lett. **40**, 1340 (1978).
- [4] L. Fleishman and P. W. Anderson, Phys. Rev. B **21**, 2366 (1980).
- [5] I. Gornyi, A. Mirlin, and D. Polyakov, Phys. Rev. Lett.

- 95**, 206603 (2005).
- [6] D. Basko, I. L. Aleiner, and B. L. Altshuler, *Ann. Phys. (N. Y.)* **321**, 1126 (2006).
- [7] N. F. Mott, *Adv. Phys.* **16**, 49 (1967).
- [8] V. Oganesyan and D. A. Huse, *Phys. Rev. B* **75**, 155111 (2007).
- [9] Y. Bar Lev and D. R. Reichman, *Phys. Rev. B* **89**, 220201 (2014).
- [10] V. Ros, M. Müller, and A. Scardicchio, *Nucl. Phys. B* **891**, 420 (2015).
- [11] M. Aizenman and S. Warzel, *Commun. Math. Phys.* **290**, 903 (2009).
- [12] J. Z. Imbrie (2014), arXiv:1403.7837.
- [13] I. Bloch and W. Zwerger, *Rev. Mod. Phys.* **80**, 885 (2008).
- [14] S. S. Kondov, W. R. McGehee, W. Xu, and B. DeMarco, *Phys. Rev. Lett.* **114**, 083002 (2015).
- [15] C. Senko, J. Smith, P. Richerme, A. Lee, W. C. Campbell, and C. Monroe, *Science* **345**, 430 (2014), arXiv:1401.5751.
- [16] A. Karahalios, A. Metavitsiadis, X. Zotos, A. Gorczyca, and P. Prelovšek, *Phys. Rev. B* **79**, 024425 (2009).
- [17] O. S. Barišić and P. Prelovšek, *Phys. Rev. B* **82**, 161106 (2010).
- [18] T. C. Berkelbach and D. R. Reichman, *Phys. Rev. B* **81**, 224429 (2010).
- [19] A. Pal and D. A. Huse, *Phys. Rev. B* **82**, 174411 (2010).
- [20] D. Thouless and S. Kirkpatrick, *J. Phys. C Solid State Phys.* **14**, 235 (1981).
- [21] O. Bohigas, M.-J. Giannoni, and C. Schmit, in *Quantum Chaos Stat. Nucl. Phys.* (1986), pp. 18–40.
- [22] G. Montambaux, D. Poilblanc, J. Bellissard, and C. Sire, *Phys. Rev. Lett.* **70**, 497 (1993).
- [23] D. Poilblanc, T. Ziman, J. Bellissard, F. Mila, and G. Montambaux, *EPL* **22**, 537 (1993).
- [24] B. N. Narozhny, A. J. Millis, and N. Andrei, *Phys. Rev. B* **58**, R2921 (1998).
- [25] F. Heidrich-Meisner, a. Honecker, and W. Brenig, *Phys. Rev. B* **71**, 184415 (2005).
- [26] F. Heidrich-Meisner, A. Honecker, and W. Brenig, *Eur. Phys. J. Spec. Top.* **151**, 135 (2007).
- [27] M. Žnidarič, T. Prosen, and P. Prelovšek, *Phys. Rev. B* **77**, 064426 (2008).
- [28] J. H. Bardarson, F. Pollmann, and J. E. Moore, *Phys. Rev. Lett.* **109**, 017202 (2012).
- [29] R. Vosk and E. Altman, *Phys. Rev. Lett.* **110**, 067204 (2013).
- [30] D. A. Huse and V. Oganesyan, arXiv:1305.4915 (2013).
- [31] M. Serbyn, Z. Papić, and D. A. Abanin, *Phys. Rev. Lett.* **111**, 127201 (2013).
- [32] R. Vasseur, S. A. Parameswaran, and J. E. Moore (2014), arXiv:1407.4476.
- [33] A. De Luca and A. Scardicchio, *EPL* **101**, 37003 (2013).
- [34] T. Giamarchi, *Quantum Physics in One Dimension* (Oxford University Press, 2004).
- [35] R. Steinigeweg and J. Gemmer, *Phys. Rev. B* **80**, 184402 (2009).
- [36] T. Prosen and M. Žnidarič, *J. Stat. Mech. Theory Exp.* **2009**, P02035 (2009).
- [37] M. Žnidarič, *Phys. Rev. Lett.* **106**, 220601 (2011).
- [38] C. Karrasch, J. E. Moore, and F. Heidrich-Meisner, *Phys. Rev. B* **89**, 075139 (2014).
- [39] S. Langer, F. Heidrich-Meisner, J. Gemmer, I. P. McCulloch, and U. Schollwöck, *Phys. Rev. B* **79**, 214409 (2009).
- [40] M. Bohm and H. Leschke, *J. Phys. A. Math. Gen.* **25**, 1043 (1992).
- [41] G. Vidal, *Phys. Rev. Lett.* **91**, 147902 (2003).
- [42] S. R. White and A. E. Feiguin, *Phys. Rev. Lett.* **93**, 076401 (2004).
- [43] E. M. Stoudenmire and S. R. White, *New J. Phys.* **12**, 055026 (2010).
- [44] S. R. White, *Phys. Rev. Lett.* **102**, 190601 (2009).
- [45] See supplemental material at [url] for a comparative analysis of the relative strengths and weaknesses of ED compare to tDMRG for the problem considered in this work.
- [46] K. Binder and W. Kob, *Glassy Materials and Disordered Solids: An Introduction to Their Statistical Mechanics* (World Scientific Publishing Company, 2005).
- [47] E. Lucioni, B. Deissler, L. Tanzi, G. Roati, M. Zaccanti, M. Modugno, M. Larcher, F. Dalfovo, M. Inguscio, and G. Modugno, *Phys. Rev. Lett.* **106**, 230403 (2011).
- [48] K. Agarwal, S. Gopalakrishnan, M. Knap, M. Müller, and E. Demler (2014), arXiv:1408.3413.
- [49] R. Vosk, D. a. Huse, and E. Altman (2014), arXiv:1412.3117.
- [50] A. C. Potter, R. Vasseur, and S. A. Parameswaran (2015), arXiv:1501.03501.
- [51] M. Schreiber, S. S. Hodgman, P. Bordia, H. P. Lüschen, M. H. Fischer, R. Vosk, E. Altman, U. Schneider, and I. Bloch (2015), arXiv:1501.05661.